Heliyon 10 (2024) e40416

Contents lists available at ScienceDirect

Heliyon

journal homepage: www.cell.com/heliyon

Research article

Characteristics of *Gracilariopsis lemaneiformis* hydrocolloids and their effects on intestine PPAR signaling and liver lipid metabolism in *Oreochromis niloticus*: A multiomics analysis

Jia-Wei Shen [a,1], Po-Kai Pan [a,1], Yin-Yu Chen [b], Fan-Hua Nan [b], Yu-Sheng Wu [a,*]

[a] *Department of Aquaculture, National Pingtung University of Science and Technology, Pingtung, 912301, Taiwan*
[b] *Department of Aquaculture, National Taiwan Ocean University, Keelung, 202301, Taiwan*

ARTICLE INFO

Keywords:
Multiomics
Genomic isoform structure
Marine algae
Hydrocolloid
Lipid metabolism

ABSTRACT

This study evaluated the effects of *Gracilariopsis lemaneiformis* hydrocolloids on Nile tilapia (*Oreochromis niloticus*) using an advanced multiomics approach (transcriptome and proteome) linked with genomic isoform structure to elucidate the biofunctions of *G. lemaneiformis* hydrocolloids. The results showed that *G. lemaneiformis* hydrocolloids did not affect growth, as indicated by the nonsignificant differences in growth and blood biochemical indicators.

Regarding the response, both intestine and liver tissues were assessed. These findings indicate that 20 % *G. lemaneiformis* hydrocolloids enhanced cytokine expression, which may contribute to a biological function in the intestine and liver of *O. niloticus*.

Genome and proteome profiles indicated that *G. lemaneiformis* hydrocolloids upregulated the intestine and liver peroxisome proliferator-activated receptor (PPAR) signaling pathway, nucleocytoplasmic transport, steroid biosynthesis, and histidine metabolism. In contrast, co-factor biosynthesis, nucleocytoplasmic transport, tryptophan metabolism, arginine and proline metabolism, arginine biosynthesis, and ribosome activity were downregulated. These findings indicate that *G. lemaneiformis* hydrocolloids significantly affect liver lipid and carbohydrate metabolism. Proteomics analysis revealed that *G. lemaneiformis* hydrocolloids upregulated the PPAR signaling pathway, playing a crucial role in lipid metabolism.

In summary, 20 % *G. lemaneiformis* hydrocolloids are primarily involved in modulating the intestine and liver PPAR signaling pathway to regulate lipid metabolism.

1. Introduction

Transcriptomics examines transcribed genetic material to analyze actively expressed genes and provide insights into cellular activities. Whereas proteomics characterizes the flow of information within cells and organisms through protein pathways and networks [1,2]. Transcriptomics assesses RNA levels genome-wide, both qualitatively and quantitatively. According to the central dogma of biology, RNA serves as a molecular intermediary between DNA and proteins, which are considered the primary functional output of DNA. RNA sequencing (RNA-Seq) studies have identified several novel isoforms, revealing a complexity in the protein-coding transcriptome greater than previously recognized [3]. Proteomics can be detected using unbiased methods such as phage display and yeast

* Corresponding author.
E-mail address: wuys0313@mail.npust.edu.tw (Y.-S. Wu).
[1] These authors contributed equally to this study.

https://doi.org/10.1016/j.heliyon.2024.e40416
Received 13 August 2024; Received in revised form 11 November 2024; Accepted 13 November 2024
Available online 20 November 2024

two-hybrid assays, or through affinity purification methods where proteins are isolated using antibodies or genetic tags adapted to explore global interactions between proteins and nucleic acids [4]. This platform offers a unique opportunity to link biological responses with chemical data in organisms exposed to environmental challenges [5].

Tilapia is a significant aquaculture product and is widely recognized as an economically important fish globally [6]. As one of the fastest-growing species in intensive farming, tilapia farming is highly productive; however, high stocking densities make both intensive and semi-intensive farms susceptible to infectious diseases [7]. The risk of outbreaks, such as Streptococcosis caused by Streptococcus agalactiae, S. dysgalactiae, S. iniae, and Lactococcus garvieae, increases with more intensive culture practices, leading to substantial economic losses [8]. Given the importance of tilapia in aquaculture, alternative health management strategies are being explored to mitigate risks and reduce negative impacts on ecosystems [9].

Recently, the biofunction of natural materials has become a significant issue, impacting both animal welfare and eco-consumerism as a means to prevent drug abuse. The use of alternative bioactive compounds as substitutes for traditional drugs is gaining global attention. Evidence suggests that marine macroalgae produce economically important polysaccharides with potential applications in pharmaceuticals, nutraceuticals, and cosmetics for health benefits [10]. For instance, Cladophora rupestris and Codium fragile are sources of bioactive compounds. Crude hydroalcoholic extracts obtained from these algae, prepared through solid/liquid extraction and fractionated via liquid/liquid purification into an ethyl acetate fraction that is rich in phenolic compounds and an aqueous fraction, exhibit antioxidant, mineralogenic, and osteogenic activities [11]. Additionally, polysaccharides from Gracilaria lemaneiformis show promise as food supplements for maintaining intestinal health in food and pharmaceutical industries [12]. Analysis of the bioactive compounds from G. lemaneiformis indicates that the extracted glucagon-like peptide 2 demonstrates wound-healing activity in animal experiments [13].

These lines of evidence suggest that G. lemaneiformis possesses biofunctions and that dietary inclusion of $<$20 % of the red algae Gracilaria arcuata does not affect the growth performance of *Oreochromis* niloticus [14]. However, the biofunction of G. lemaneiformis hydrocolloids remains unclear, particularly concerning physiological systems. This study aimed to investigate the effects of 5 %, 10 %, and 20 % G. lemaneiformis hydrocolloids on the growth of *O. niloticus* and analyze hematological parameters to assess the safety of these extracts. Additionally, intestinal and liver immune responses were examined based on cytokine expression levels and histological analysis was performed to evaluate the biofunctional role of G. lemaneiformis hydrocolloids.

Furthermore, we compared transcriptome profiles of the liver and intestine between a nondietary intervention and a diet containing 20 % G. lemaneiformis hydrocolloids and examined genome isoform structures to elucidate mRNA expression mechanisms. Finally, we evaluated the biofunction of G. lemaneiformis hydrocolloids in the liver through proteomic analysis, focusing on molecular interactions at the protein level.

2. Materials and methods

2.1. Fish rearing conditions

Approximately 10 g *O. niloticus* fish were obtained from Sheng-Diao Aquatic Technology, Pingtung, Taiwan. The fish were randomly selected and transported to the laboratory in fish bags with pure oxygen. Upon arrival, their feeding behavior, swimming activity, and body color were monitored as indicators of health. Once the fish were acclimated to the experimental water conditions, the experiments were commenced. The cultured water environment was maintained at 25 °C (pH 7.5).

2.2. G. lemaneiformis hydrocolloid preparation

G. lemaneiformis was obtained from aquaculture practitioner Tzu-Yu Tseng (Yilan, Taiwan). Hydrocolloids were extracted from 20 g of dried G. lemaneiformis mixed with 1000 mL distilled water under 60 °C for 16 h. After, the extraction residue was removed via centrifugation (5000 rpm) for 1 h, and the supernatant was collected as hydrocolloids [15]; [63].

2.3. Experimental diets and design

The diet was prepared based on commercial tilapia feed (SHYE YIH FEEDING). The basal feed composition was approximately 11 % water, 25 % crude protein, 3 % crude lipid, 16 % ash, and 6.5 % crude fiber. *G. lemaneiformis* water extract was sprayed onto the commercial feed. The prepared feeds contained 0 %, 5 %, 10 %, and 20 % *G. lemaneiformis* water extract per kilogram.

The daily feed intake for Nile tilapia was set at 5 % of their body weight. Five individuals per group were used, and the experiments were performed thrice.

Feeding trials were conducted over a period of 4 weeks. The survival rate of the fish throughout the experiment was 100 %. Each week, the body weight and length of the tilapia were measured. At the end of the experiment, the tilapia were euthanized, and the liver, spleen, intestine, and peripheral blood were collected. The collected liver and spleen were weighed and compared with the body weight, with results presented as hepato-somatic (Liver Weight (Final)/Body Weight) and spleen-somatic (Spleen Weight (Final)/Body Weight) indices.

Table 1
Primers used for qPCR.

Gene	Forward primer	Reverse primer	Reference/Gene bank No.
β-actin	TCCTTCCTTGGTATGGAATCC	GTGGGGCAATGATCTTGATC	KJ126772
IL-1β	CAGTGAAGACCGCAAAGTGC	TATCCGTCACCTCCTCCAG	XM_019365841
TNF-α	GAACACTGGCGACAAAACAGA	TTGAGTCGCTGCCTTCTAGA	AY428948
IL-10	GAAGAGAGATGTCACCCAGTGTAGG	TCTTGATTTGGGTCAGCAGGTC	XM_003441366. 3

2.4. Growth index formulas

Feed conversion ratio (FCR) = feed intake/weight gain

Average daily gain (ADG, g) = weight gain/number of days on feed

Specific growth rate (SGR, %/day) = [(ln Wt $_{(final)}$) − (ln $Wt_{(initial)}$)/T(days)] x 100.

Condition factor (K, g/cm^3) = weight/length^3 [16]

3. Blood sample

3.1. Hematological parameters

At the end of the feeding period, five individuals (average weight: approximately 30 g) per group were selected from each experimental tank. The experiments adhered to the guidelines provided by the Council of Agriculture Executive Yuan, Taiwan, for the Care and Use of Laboratory Animals. To reduce fish activity, they were placed in ice-chilled water at 2–4 °C for 20 min. Blood samples (1 mL) were then collected from the caudal vessels using heparinized syringes and transferred to sterile tubes for biochemical analysis. Hemolyzed, clotted, or insufficient samples were discarded. Plasma samples were analyzed for glucose [17], total cholesterol (T-cho), blood urea nitrogen (BUN), total bilirubin (T-Bil), aspartate aminotransferase (GOT), alanine aminotransferase (GPT), total protein (T-pro), albumin (Alb), calcium (Ca), triglycerides (TGs), creatine phosphokinase (CPK), uric acid (UA), and lactate dehydrogenase (LDH) using an automated blood biochemical analyzer (SPOTCHEM, EZ SP-4430, ARKRAY, Japan).

3.2. Blood cell counting

Blood samples (1 mL) were collected from the caudal vessels using heparinized syringes and placed in sterile tubes for total cell counting. The samples were analyzed using the LUNA™ FL Dual Fluorescence Cell Counter.

4. Tissue sample

4.1. Liver and intestine immune gene expression

Real-time reverse transcription quantitative PCR (qPCR) was performed to analyze immune gene expression in liver and intestinal tissue samples. The samples were sent to Genomics, Taiwan, for real-time qPCR analysis of interleukin (IL)-1β, tumor necrosis factor (TNF)α, and IL-10. β-Actin was used as the reference gene in the comparative cycle threshold (CT) method to determine relative expression levels. Fluorescence was analyzed using the auto-CT method to set the threshold for each gene, and the $2^{-\Delta\Delta CT}$ method was used to calculate CT values. Data are presented as fold changes in mRNA levels relative to the reference gene β-actin. The oligonucleotide sequences used as qPCR primers are listed in Table 1 [18,19].

4.2. Histological analysis

Intestine, liver, and spleen tissues were fixed in 10 % formalin. The liver tissues were then embedded in paraffin, sectioned at 5 μm thickness, and stained with hematoxylin–eosin (HE) and Giemsa. These stained sections were analyzed using microscopy.

5. Transcriptome

5.1. Liver and intestine RNA-Seq

For RNA-Seq analysis, liver and intestine samples were collected from both nondietary and 20 % G. lemaneiformis hydrocolloid diet groups. Each pooled tissue sample consisted of five individual samples combined into a single library. Thus, there were two libraries for liver samples (control and 20 % diet) and two libraries for intestine samples.

A.

	Con	5%	10%	20%
Initial length (cm)	6.3 ± 0.35	6.27 ± 0.32	6.34 ± 0.17	6.15 ± 0.32
Final length (cm)	10.38 ± 1.07	9.72 ± 0.5	9.82 ± 0.45	9.52 ± 0.43
Initial weight (g)	9.97 ± 0.66	9.65 ± 0.59	9.89 ± 0.68	9.35 ± 0.72
Final weight (g)	33.53 ± 5.01	29.54 ± 5.69	31.76 ± 5.42	28.44 ± 4.01
ADG ($g\ d^{-1}$)	1.02 ± 0.1	0.86 ± 0.04	0.95 ± 0.06	0.82 ± 0.04
SGR ($\%\ d^{-1}$)	1.94 ± 0.08	1.79 ± 0.04	1.87 ± 0.11	1.78 ± 0.07
Condition factor ($g\ cm^{-3}$)	3.03 ± 0.57	3.21 ± 0.16	3.35 ± 0.15	3.28 ± 0.07
FCR	4.00 ± 0.21	4.48 ± 0.16	4.38 ± 0.34	4.63 ± 0.31

B.

	Con	5%	10%	20%
Liver-Body ratio (%)	1.07±0.15	1.21±0.49	1.46±0.35	1.53±0.57
Spleen-Body ratio (%)	0.16±0.13	0.25±0.16	0.23±0.11	0.19±0.09
BTCC (Blood Total Cell Counts) (cells/ml)	$4.62x10^{8}$±$7.61x10^{8a}$	$8.07x10^{8}$±$2.75x10^{8ab}$	$1.2x10^{9}$±$3.34x10^{8ab}$	$1.5x10^{9}$±$5x10^{8b}$
Average Size (μm)	7.2±1.12	7.46±0.68	6.9±0.57	7.12±1.06
Glu (mg/dl)	116.8±22.55	117.6±24.84	123.4±39.34	106.8±39.04
T-Cho (mg/dl)	256±62.11	215±27.99	317.4±85.75	269.6±97.04
BUN (mg/dl)	~5	~5	~5	~5
T-Bil (mg/dl)	0.54±0.46	0.36±0.15	0.44±0.17	0.38±0.19
GOT (IU/L)	209±158.53	131±51.64	159.8±68.21	190.2±156.82
GPT (IU/L)	59±36.04	43±5.13	67±18.71	69±34.12
T-Pro (g/dl)	2.78±0.39	2.86±0.6	2.9±0.34	2.82±0.33
Alb (g/dl)	~1	~1	~1	~1
Ca (mg/dl)	18.14±0.86	16.7±3.35	17.44±0.91	17.92±1.01
TG (mg/dl)	82.4±21.04	116±39.49	121.4±74.12	126±44.35
UA (mg/dl)	1.74±1.07	1.12±0.27	1.18±0.35	1.42±0.58
LDH (IU/L)	2564±1730.0	2795.4±1124.7	2900±1029.8	2717.6±1043.3

(C)

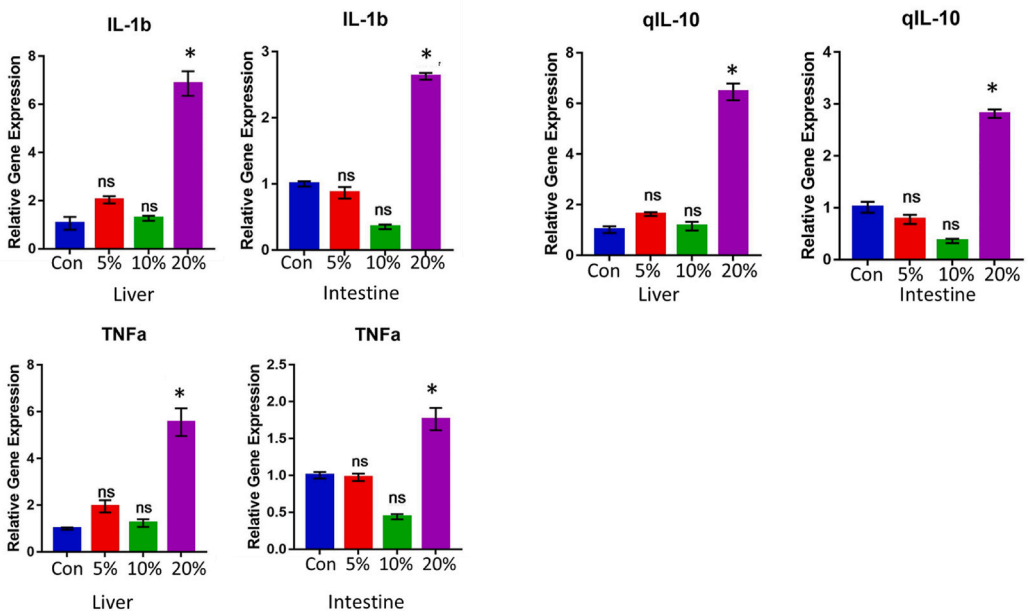

Fig. 1. Effects of dietary *G. lemaneiformis* hydrocolloids on the growth, hematological, immune gene expression, and histological characteristics of *O. niloticus*.

(A). Growth indices: feed conversion ratio (FCR); average daily gain (ADG, g); specific growth rate (SGR, %/day); condition factor (K, g/cm).

(B). Hematological characteristics: Each value represents the mean ± SEM (n = 5). Data were considered statistically significant at $p < 0.05$ and are indicated with different letters (a, b).

(C). Gene expression: IL-1β, TNF-α, and qIL-10 expression in the *O. niloticus* intestine and liver. Each value represents the mean ± SEM (n = 5). Data were considered statistically significant relative expression higher or lower two times more than control was marked as *, less was marked as non-significant (ns).

(D). Histological characteristics. Liver tissue leukocyte infiltration is indicated by red arrows. Goblet cells in the intestine are indicated by red arrows. Black scale bar = 50 μm. (For interpretation of the references to color in this figure legend, the reader is referred to the Web version of this article.)

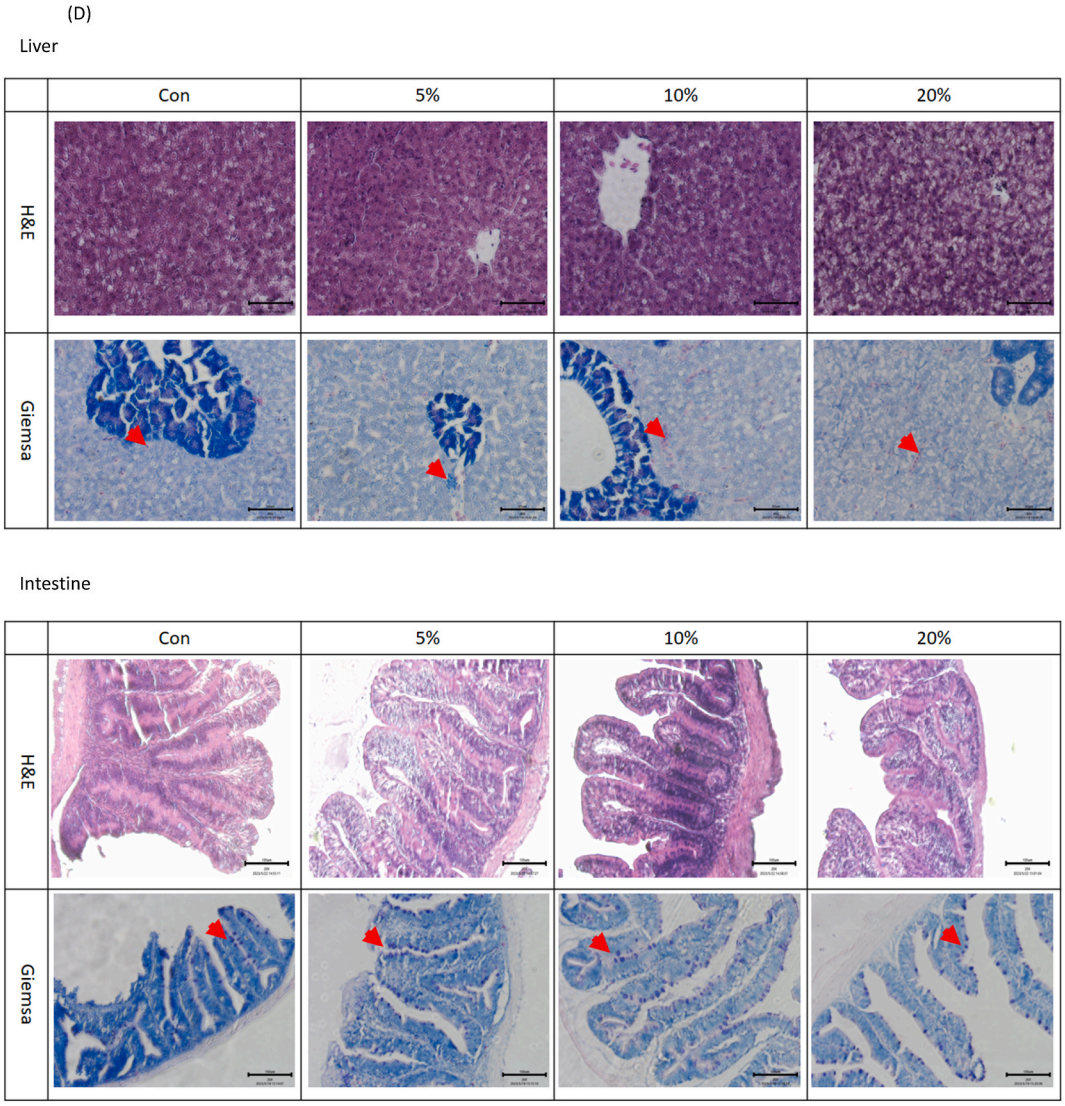

Fig. 1. (*continued*).

RNA was isolated from the tissues using QIAzol lysis reagent (Qiagen). RNA concentrations were measured using a Nanodrop spectrophotometer. Subsequently, 1 μg of RNA from each sample was sent to Biotools Co., Ltd., Taiwan, for RNA-Seq (transcriptome) analysis using the NovaSeq 6000 Sequencing System (Illumina).

For library construction, quality control, and sequencing, a de novo analysis approach was employed. mRNA was purified from total RNA using poly-T oligo-attached magnetic beads. After fragmentation, first-strand cDNA was synthesized with random hexamer primers, followed by the synthesis of second-strand cDNA. dUTP was used for directional libraries, whereas dTTP was used for nondirectional libraries. Nondirectional libraries were subjected to end repair, A-tailing, adapter ligation, size selection, amplification, and purification. Transcriptome assembly was performed using Trinity, a professional software for transcriptome assembly comprising modules named Inchworm, Chrysalis, and Butterfly. The workflow for Trinity can be found at http://trinityrnaseq.github.io/. To remove redundancy from the Trinity results, CORSET software was used. Hierarchical clustering was performed based on multiple mapping events and expression patterns. The CORSET workflow can be found at https://github.com/Oshlack/Corset/wiki. Finally, BUSCO was used to assess the completeness of the transcriptome in terms of expected gene content.

5.2. *Liver proteomic analysis*

Liver samples from tilapia were sent to Biotools Co., Ltd., Taiwan, for proteomic analysis. Proteins were first extracted and quantified using a protein BCA assay kit (Thermo). The protein solutions were diluted in 50 mM ammonium bicarbonate (Sigma), reduced with 10 mM dithiothreitol (Merck) at 56 °C for 45 min, and then cysteine-blocked with 50 mM iodoacetamide (Sigma) at 25 °C

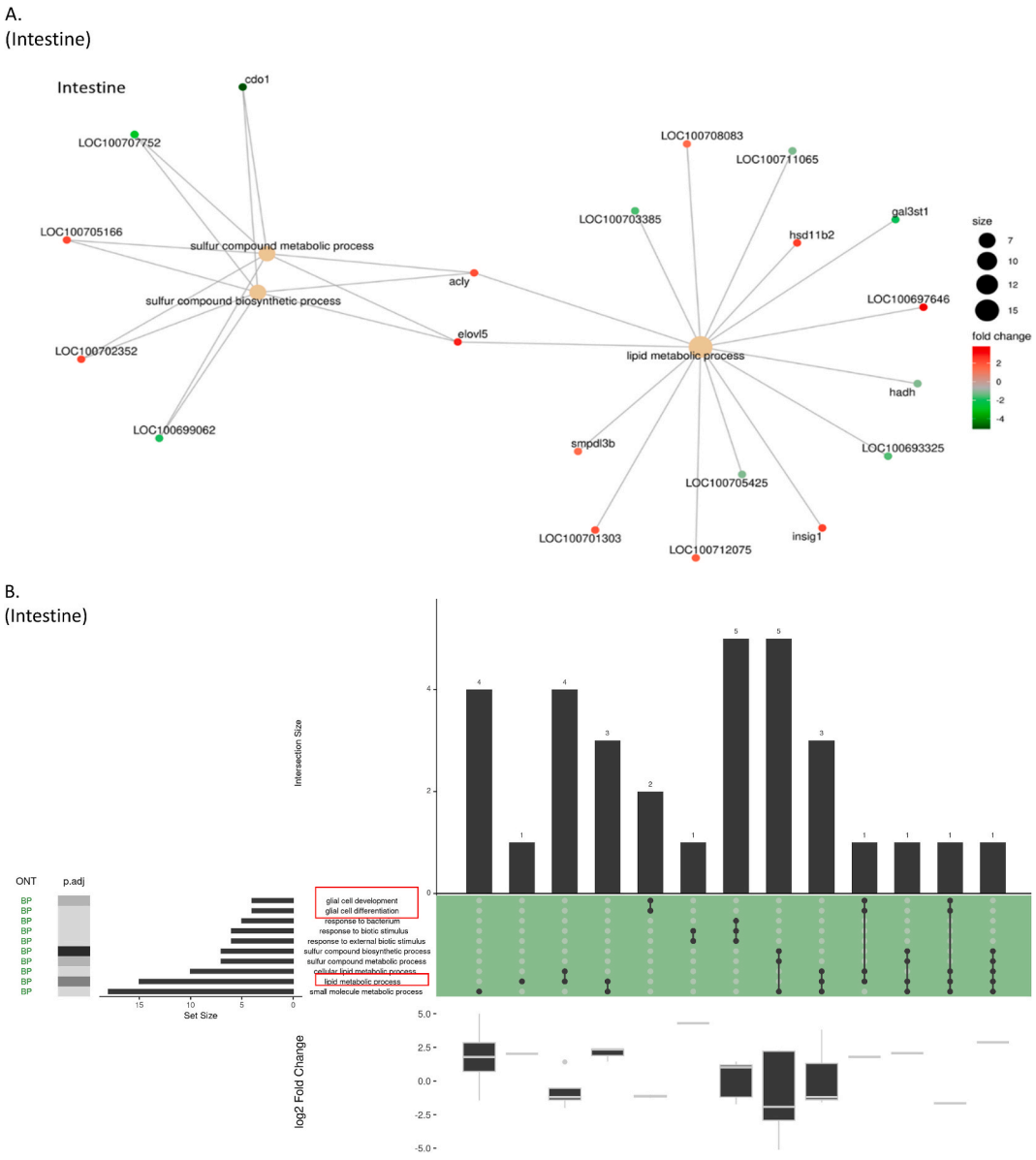

Fig. 2. Transcriptomic analysis of dietary *G. lemaneiformis* hydrocolloids in *O. niloticus* intestine: upregulated and downregulated gene expression of GO terms and KEGG pathways.
(A). Relationship of detected gene expressions: Red spots indicate upregulated genes, whereas blue spots indicate downregulated genes.
(B). Analysis of BP, CC, and MF: major biofunctions affected by *G. lemaneiformis* hydrocolloids.
(C). Functional linkage: bifunctional relationships of *G. lemaneiformis* hydrocolloids in *O. niloticus* intestine KEGG pathways. (For interpretation of the references to color in this figure legend, the reader is referred to the Web version of this article.)

for 30 min. The samples were stored at −80 °C until use. The digested peptides were diluted in HPLC buffer A (0.1 % formic acid) and loaded onto a reverse-phase column (Zorbax 300SB-C18, 0.3 × 5 mm; Agilent Technologies). Desalted peptides were separated on a column (Waters BEH 1.7 μm, 100 μm I.D. × 10 cm with a 15 μm tip) using a multistep gradient of HPLC buffer B (99.9 % acetonitrile/ 0.1 % formic acid) for 70 min at a flow rate of 0.3 μL/min. Data-dependent MS/MS scans were performed, with one MS scan followed by MS/MS scans of the 20 most abundant precursor ions detected in the preview MS scan. Automatic gain control settings were 1000 ms for full scans and 200 ms for MS/MS scans or 3×10^6 ions for full scans and 3000 ions for MS/MS, respectively. Data analysis was conducted using Proteome Discoverer software (version 2.3, Thermo Fisher Scientific). MS/MS spectra were searched against the UniProt database using the Mascot search engine (Matrix Science, London, UK; version 2.5).

C.
(Intestine)

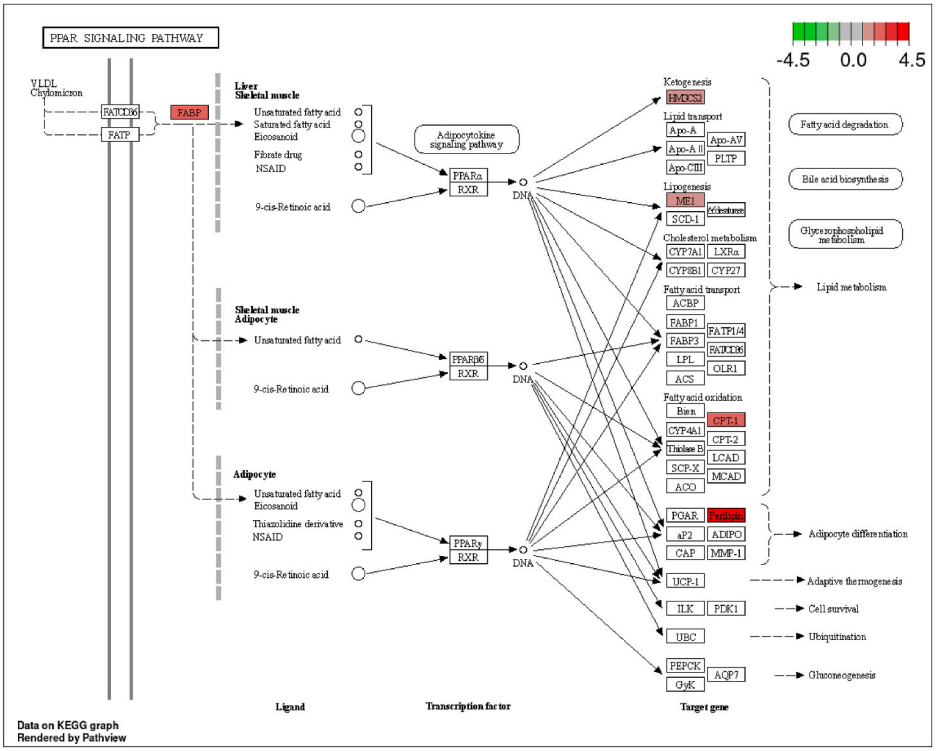

Fig. 2. (*continued*).

5.3. Statistical analysis

Statistical significance of differences in growth and blood biochemical indicators between the treatment and control groups was assessed using one-way analysis of variance and Scheffe's test, with significance set at $p < 0.05$. Results are presented as mean ± standard deviation. In the gene expression, the relative expression higher or lower two times more than control was thought as significant marked as *, less was marked as non-significant (ns). Differential proteins were identified using a threshold defined as the mean of the $\log_2$ transformed ratio ±1 × standard deviation of the $\log_2$ transformed ratio, assuming a normalized distribution of the ratio.

6. Results

6.1. Growth and hematological parameters

To determine the impact of *G. lemaneiformis* hydrocolloids on experimental animals, we assessed their effects on the growth performance and hematological parameters of Nile tilapia. Fig. 1A presents data on weight, length, ADG, SGR, K, and FCR over a 4-week feeding period with *G. lemaneiformis* hydrocolloids. The initial weights of the fish were 9.97 ± 0.66 g (control), 9.65 ± 0.59 g (5 % hydrocolloids), 9.89 ± 0.68 g (10 % hydrocolloids), and 9.35 ± 0.72 g (20 % hydrocolloids), with no significant differences among the groups ($p > 0.05$). After 4 weeks, the final weights were 33.53 ± 5.01 g (control), 29.54 ± 5.69 g (5 % hydrocolloids), 31.76 ± 5.42 g (10 % hydrocolloids), and 28.44 ± 4.01 g (20 % hydrocolloids), with no significant differences among the groups ($p > 0.05$). Furthermore, the fish length, ADG, SGR, K, and FCR showed no significant differences compared with the control group ($p > 0.05$).

Feeding with *G. lemaneiformis* hydrocolloids did not result in significant differences in hepato-somatic and spleen-somatic ratios after 4 weeks ($p > 0.05$). Total blood cell counts revealed that the addition of 20 % *G. lemaneiformis* hydrocolloids increased cell counts compared with the control group ($p < 0.05$). However, blood biochemical analysis showed no significant differences in the levels of glucose, T-cho, BUN, T-Bil, GOT, GPT, T-pro, Alb, Ca, TGs, CPK, UA, and LDH between the experimental groups ($p > 0.05$) (Fig. 1B).

In the initial experiment, *G. lemaneiformis* hydrocolloids did not show improvements in growth or alter hematological parameters. Consequently, we conducted histological observations to examine changes in major digestive tissues, specifically the liver and intestine. We also assessed tissue-related immune genes, including those encoding for IL-1β, TNF-α, and IL-10.

Feeding *O. niloticus* with *G. lemaneiformis* hydrocolloids induced IL-1β, TNF-α, and IL-10 gene expression in both the liver and intestine (Fig. 1C). Compared to the control, IL-1β levels were significantly higher in the liver and intestine of the 20 % group. However, IL-1β levels in the intestine were significantly reduced in the 10 % group. Additionally, TNF-α levels were significantly elevated in the liver and intestine of the 20 % group compared with the other groups. Similarly, IL-10 levels were significantly

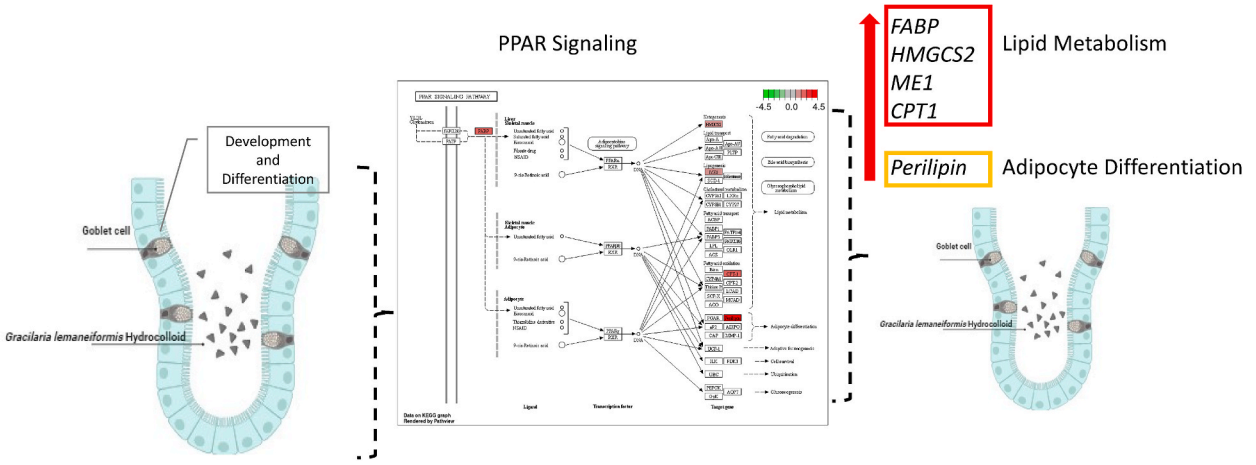

Fig. 3. Summary of the *G. lemaneiformis* hydrocolloids function in *O. niloticus* intestine PPAR Signaling pathway which related to lipid metabolism and adipocyte differentiation.

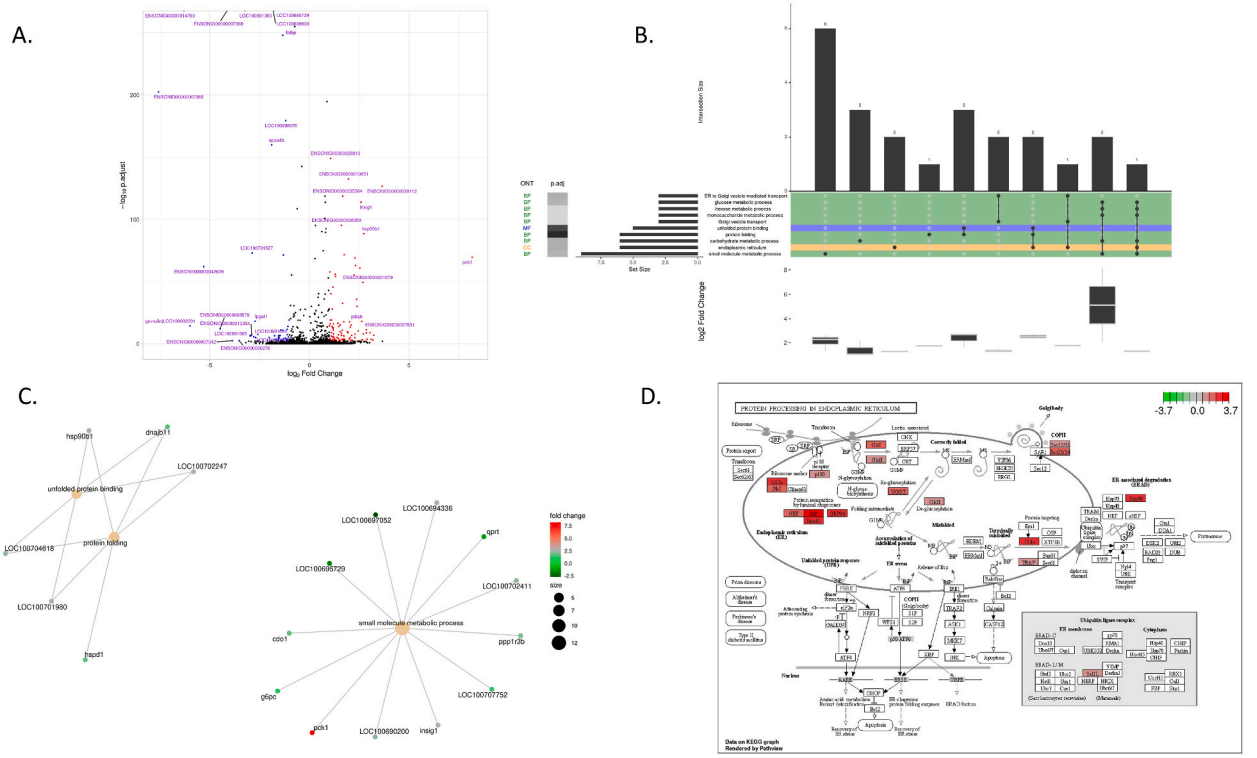

Fig. 4. Transcriptomic analysis of dietary *G. lemaneiformis* hydrocolloids in *O. niloticus* liver: GO terms and KEGG pathways.
(A). Relationship of detected gene expressions: Red spots indicate upregulated genes, whereas blue spots indicate downregulated genes.
(B). Analysis of BP, CC, and MF: major biofunctions affected by *G. lemaneiformis* hydrocolloids.
(C). Functional linkage: bifunctional relationships of *G. lemaneiformis* hydrocolloids in *O. niloticus* liver.
(D). KEGG pathways affected by *G. lemaneiformis* hydrocolloids in *O. niloticus* liver. (For interpretation of the references to color in this figure legend, the reader is referred to the Web version of this article.)

increased in both the liver and intestine of the 20 % group.

O. niloticus fed with *G. lemaneiformis* hydrocolloids exhibited normal liver tissue structure and morphology as demonstrated via HE staining (Fig. 1D). However, Giemsa staining revealed leukocyte infiltration in the liver tissue (red arrow). The intestine of fish fed with *G. lemaneiformis* water extract also showed normal tissue structure, as evidenced via HE staining (Fig. 1D), but Giemsa staining indicated an increased number of goblet cells in the intestine (red arrow).

A.

Sample	Protein ID (No.)	Peptide ID (No.)	Search input (No.)	20%/Con				
				Total Quant No.	≥ mean+1×SD	≤ mean-1×SD	Up-regulated pathway	Down-regulated pathway
Con	739	4991	17596					
20%	594	3755	16585	806	41	55	7	7

B.

		(20%) / (Con)							
Category	Trend	Term	Count	Genes	%	PValue	Benjamini	FDR	Fold Enrichment
KEGG-pathway	Up-regulate	onl03320:PPAR signaling pathway	3	A0A669C1T4, I3KDH3, A0A669D0M9	5.55555	0.03056	0.49934	0.49934	10.47299509
		onl03013:Nucleocytoplasmic transport	3	I3KMP5	5.55555	0.04697	0.49934	0.49934	8.272786037
		onl01100:Metabolic pathways	11	A0A669BDR4, I3KUV8, D2KP27, A0A669DS56, I3J0B7, A0A669BSA0, A0A669EYY8, A0A669C1T4, I3K9H9, A0A669CU46, A0A669E7L0	20.37037	0.054612	0.499346	0.499346	1.7685901
		onl00900:Terpenoid backbone biosynthesis	2	A0A669C1T4, A0A669CU46	3.70370	0.06534	0.49934	0.49934	28.53511706
		onl00340:Histidine metabolism	2	A0A669BSA0, A0A669EYY6	3.70370	0.08440	0.53055	0.53055	21.87692308
	Down-regulate	onl01240:Biosynthesis of cofactors	6	I3KDB1, I3K4Z7, A0A669B336, A0A669BMG9, I3JPY1, I3J5I1	9.67741	7.56E-04	0.03211	0.03211	7.874480849
		onl01100:Metabolic pathways	17	I3KF61, A0A669B336, A0A669DA03, I3JPY1, A8WE65, I3JN99, A0A669DDJ1, I3KDB1, I3K4Z7, I3IUQ2, A0A669DQP1, A0A669EGE5, A0A669BMG9, A0A669BYN1, I3KQD0, I3J5I1	27.41935	0.001189	0.032115	0.032115	2.1534898
		onl03013:Nucleocytoplasmic transport	4	A0A669CLM6, A0A669CEL7, A0A669B869	6.45161	0.00977	0.17593	0.17593	8.690603514
		onl00380:Tryptophan metabolism	3	A0A669EGE5, A0A669BMG9, I3JPY1	4.83870	0.02041	0.27559	0.27559	13.14637904
		onl00330:Arginine and proline metabolism	3	I3IUQ2, I3JPY1, A0A669BYN1	4.83870	0.02735	0.29538	0.29538	11.24110672
		onl00220:Arginine biosynthesis	2	I3IUQ2, A0A669BYN1	3.22580	0.09661	0.76149	0.76149	19.15151515
		onl03010:Ribosome	3	A0A669B4T4, I3JMG5	4.83870	0.09871	0.76149	0.76149	5.462227913

C.

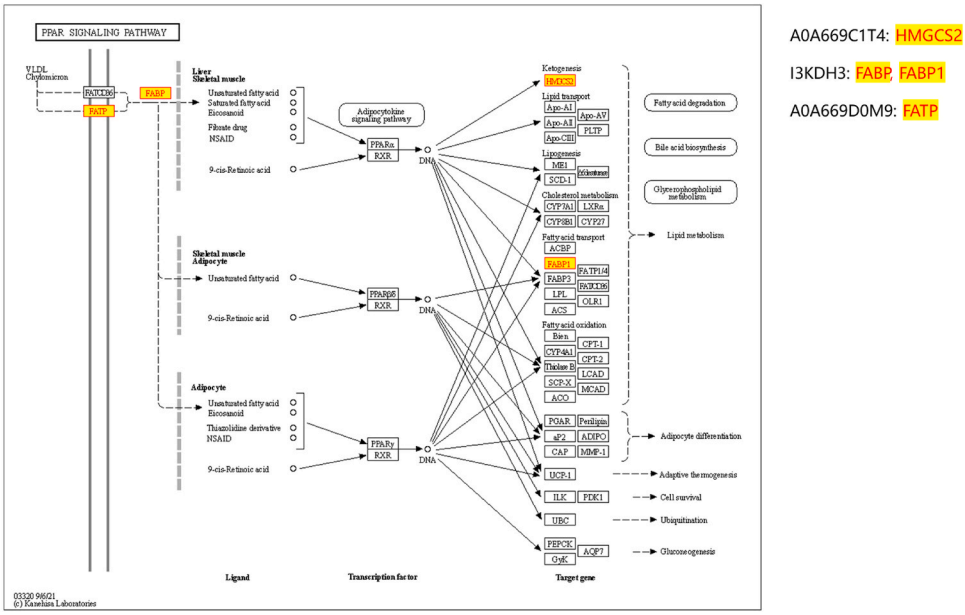

Fig. 5. Characteristics of the biofunctions of *G. lemaneiformis* hydrocolloids in *O. niloticus* liver determined through proteomic analysis.
(A). Number of detected proteins compared with the control.
(B). Upregulated and downregulated proteins related to the bioregulation response.
(C). KEGG pathways illustrating the biofunction of *G. lemaneiformis* hydrocolloids in liver lipid metabolism in *O. niloticus*.

These results indicate that feeding *O. niloticus* with 5 %, 10 %, and 20 % *G. lemaneiformis* hydrocolloids in the tissues, particularly by increasing the number of goblet cells in the intestine. Although these dietary supplements did not enhance juvenile growth or negatively impact the fish, as evidenced through blood biochemical analysis.

6.2. *G. lemaneiformis hydrocolloids affected the intestinal TNF signaling pathway*

Generally, GO terms with an adjusted P-value of <0.05 were considered significantly enriched. In GO terms, **molecular function** (MF) refers to cellular activities at the molecular level, **biological process (BP)** denotes the biological goals and functions accomplished by these activities, and **cellular component (CC)** pertains to the subcellular structures and macromolecular complexes where these processes occur.

In the intestine, results indicated that *G. lemaneiformis* hydrocolloids specifically regulated sulfur compound biosynthesis and metabolic processes associated with *cdo1* (Fig. 2A). *G. lemaneiformis* hydrocolloids predominantly influenced BPs, including glial cell development and differentiation, and lipid metabolism (Fig. 2B). From transcriptome analysis, *G. lemaneiformis* hydrocolloids were shown to enhance the intestinal *FABP, HMGCS2, ME1* and *CPT1*, which was corresponding to PPAR signaling pathway in Kyoto Encyclopedia of Genes and Genomes (KEGG) database (Fig. 2C).

In summary, *G. lemaneiformis* hydrocolloids induce the intestinal *FABP, HMGCS2, ME1* and *CPT1* expression, which was thought to regulate the lipid metabolism and adipocyte differentiation (Fig. 3).

6.3. *G. lemaneiformis hydrocolloids affected the Liver's endoplasmic reticulum protein processing*

GO analysis revealed that *G. lemaneiformis* hydrocolloids primarily affected liver protein folding processes, involving genes such as ***hspd1***, ***hsp90b1***, and others. Additionally, they regulated small molecule metabolic processes, linked to genes such as ***ppp1r3b***, ***insig1***, ***pck1***, and ***g6pc*** (Fig. 4A and B).

Through the analysis of gene linkages, we distinguished the major roles of *G. lemaneiformis* hydrocolloids in Nile tilapia by examining BP, CC, and MF terms.

Specifically, the hydrocolloids were found to regulate protein folding within BP and the endoplasmic reticulum within CC in the liver, as evidenced by the enhanced expression (Fig. 4C and D).

KEGG pathway analysis showed that *G. lemaneiformis* hydrocolloids enhanced protein processing in the endoplasmic reticulum in the liver, which is crucial for protein structure modification and correction.

6.4. *Functions of G. lemaneiformis hydrocolloids in liver lipid metabolism*

The effects of *G. lemaneiformis* hydrocolloids on liver proteomics have not been previously reported. This study aimed to assess the liver proteome profile to identify significant changes in liver structure and function following the administration of *G. lemaneiformis* hydrocolloids. Nile tilapia were fed diets containing 0 %, 5 %, 10 %, and 20 % *G. lemaneiformis* hydrocolloids. The 20 % treatment exhibited the most pronounced effects on the fish. Based on these findings, we selected the 20 % *G. lemaneiformis* hydrocolloid group for further analysis of liver proteome alterations.

In proteomic analysis, a total of 17,596 proteins were identified in the control group, whereas 16,585 proteins were identified in the 20 % treatment group. Compared with the control, 806 proteins showed differential expression. Functional annotation of these proteins revealed that five pathways were significantly upregulated, whereas seven pathways were downregulated (Fig. 5A).

In the upregulated protein analysis, 41 proteins were found to be significantly upregulated compared with the control, including 60S ribosomal protein L27, histamine N-methyltransferase, coatomer subunit beta, ribosomal protein L5, uncharacterized LOC100697673, apolipoprotein A-I, protein phosphatase 2, regulatory subunit A, beta a, solute carrier family 2, facilitated glucose transporter member 2, choline dehydrogenase, fetuin-B, superoxide dismutase [Mn] mitochondrial, mesencephalic astrocyte-derived neurotrophic factor, C-type lectin domain-containing protein, cytochrome P450, family 51, cytochrome P450, family 2, and fatty acid-binding protein [20], among others (Fig. 5B). These proteins were primarily associated with several KEGG pathways: primary bile acid biosynthesis (35-fold enrichment), peroxisome proliferator-activated receptor (PPAR) signaling pathway (10-fold enrichment), nucleocytoplasmic transport (8-fold enrichment), metabolic pathways (1.7-fold enrichment), terpenoid backbone biosynthesis (28-fold enrichment), steroid biosynthesis (27-fold enrichment), and histidine metabolism (21-fold enrichment).

In the downregulated protein analysis, 55 proteins were found to be significantly reduced compared with the control, including tubulin beta chain, microtubule-associated protein, GOT, phosphoenolpyruvate carboxykinase (GTP), ADP-ribosylation factor 2b, heterochromatin protein 1, binding protein 3, SEC31 homolog A, COPII coat complex component, glucose-6-phosphate 1-dehydrogenase, coatomer subunit gamma, ribonucleoprotein, protein disulfide isomerase family A member 5, tubulin/FtsZ GTPase domain-containing protein, multifunctional fusion protein, Ras-related protein Rab-1A, annexin, T-complex protein 1 subunit beta, carboxypeptidase, sulfotransferase, dimethylargininase, ribosomal protein L12, enoyl-CoA hydratase, retinol dehydrogenase 11, and retinol dehydrogenase 13, among others. These proteins were associated with several KEGG pathways: biosynthesis of cofactors (7-fold enrichment), metabolic pathways (2-fold enrichment), nucleocytoplasmic transport (8-fold enrichment), tryptophan metabolism (13-fold enrichment), arginine and proline metabolism (11-fold enrichment), arginine biosynthesis (19-fold enrichment), and ribosome (5-fold enrichment). Notably, these metabolic pathways appeared in both upregulated and downregulated KEGG results. Specifically, 11 proteins were upregulated in these pathways, whereas 17 proteins were downregulated (Fig. 5B).

Following this, we performed KEGG analysis to evaluate the detected proteins. We found that that *G. lemaneiformis* hydrocolloids

Table 2
Liver transcriptome and proteome of *O. niloticus* after feeding with *G. lemaneiformis* hydrocolloids.

Liver	Transcriptome	Proteome
Up-regulate	phosphoenolpyruvate carboxykinase 1 (log2fold change = 8.16)	Ketohexokinase (Normalized ratio = 81.73)
	endoplasmic reticulum chaperone BiP (log2fold change = 3.66)	Moesin (Normalized ratio = 81.73)
	transcriptional regulator Myc-A (log2fold change = 3.23)	Cytochrome *c* oxidase subunit 5A (Normalized ratio = 81.73)
	DNA damage-inducible transcript 4 protein (log2fold change = 3.18)	24-dehydrocholesterol reductase (Normalized ratio = 81.73)
	PTC7 protein phosphatase homolog (log2fold change = 3.04)	Solute carrier family 27 member 2a (Normalized ratio = 81.73)
	28S ribosomal RNA (log2fold change = 2.90)	Epoxide hydrolase (Normalized ratio = 81.73)
	circadian associated repressor of transcription a (log2fold change = 2.90)	Alpha-2-macroglobulin-like (Normalized ratio = 81.73)
	acyl-CoA desaturase (log2fold change = 2.87)	Elongation factor 1-alpha (Normalized ratio = 50.47)
	complement C1q-like protein 3 (log2fold change = 2.86)	Ubiquinol-cytochrome c reductase core protein 1 (Normalized ratio = 18.14)
	heat shock protein 90 beta family member 1 (log2fold change = 2.73)	Hydroxymethylglutaryl-CoA synthase (Normalized ratio = 12.75)
Down-regulate	vitellogenin-1 (log2fold change = −7.58)	Arginase (Normalized ratio = 0.24)
	granulins (log2fold change = −5.99)	Galectin (Normalized ratio = 0.24)
	cathepsin E-A (log2fold change = −5.30)	Dehydrogenase/reductase SDR family member 13 (Normalized ratio = 0.24)
	extracellular serine/threonine protein kinase FAM20C (log2fold change = −4.47)	Nicotinate-nucleotide pyrophosphorylase [carboxylating] (Normalized ratio = 0.24)
	vitellogenin (log2fold change = −3.22)	Cytochrome P450 2K1-like (Normalized ratio = 0.23)
	choline-phosphate cytidylyltransferase B (log2fold change = −2.97)	Kynureninase (Normalized ratio = 0.21)
	cyclin-G2 (log2fold change = −2.93)	Large ribosomal subunit protein eL38 (Normalized ratio = 0.21)
	estrogen receptor 1 (log2fold change = −2.89)	Actin, cytoplasmic 1 (Normalized ratio = 0.21)
	cytochrome P450 2J2 (log2fold change = −2.86)	Cytochrome P450, family 3, subfamily A, polypeptide 65 (Normalized ratio = 0.21)

significantly affected liver PPAR signaling, primarily upregulating pathways related to lipid metabolism. This finding indicates that the hydrocolloids play a crucial role in lipid metabolism (Fig. 5C).

Combining the liver transcriptomic and proteomic analysis results, we observed that the upregulated genes *Bip*, *Hsp40*, *GRF94*, and *NEF* are associated with protein recognition by luminal chaperones at the molecular level. At the protein level, key molecules involved in liver lipid metabolism, such as 3-hydroxy-3-methylglutaryl-CoA synthase 2 (HMGCS2), FABP, FABP1, and FATP, which are crucial for fatty acid degradation, were found to be upregulated (Table 2).

7. Discussion

In this study, we found that *G. lemaneiformis* water extract did not cause damage to liver or intestinal tissues, as confirmed via hematological and histological analyses. However, the extract significantly increased the expression of IL-1β, TNF-α, and IL-10 genes in both liver and intestine, indicating that *G. lemaneiformis* water extract plays a role in regulating physiological responses. Based on preliminary experiments, the 20 % treatment exhibited the most significant effects. Consequently, we analyzed the liver and intestine by performing full-length sequencing and transcriptome analysis to explore molecular interactions and employed LC-MS/MS to evaluate liver proteome expression.

A previous study showed that supplementing fishmeal with 10 % *Porphyra dioica* or *Ulva* spp. in the diet of *O. niloticus* juveniles did not negatively impact growth performance or body composition; however, a 10 % inclusion of *Gracilaria vermiculophylla* in the diet reduced feed intake and growth performance in *O. niloticus* juveniles [21]. Another study found that supplementing fishmeal with <20 % of the red alga *Gracilaria arcuata* did not affect the growth performance of *O. niloticus* [14].

According to material analysis, *Gracilaria* species produce lectins that are resistant to fish digestive proteolytic enzymes and can reduce gut nutritional digestion [22]. Consistent with these findings, our study showed that feeding *O. niloticus* juveniles 5 %, 10 %, and 20 % *G. lemaneiformis* water extract for 30 days had no adverse effects on fish growth. The observed ADG, SGR, K, and FCR values were comparable to those reported by Bardocz et al. [22]. Therefore, we infer that *G. lemaneiformis* water extract may not serve as an energy source but might influence other physiological functions in *O. niloticus* juveniles. To further explore this, we subsequently examined hematological parameters.

Plasma levels of GOT and GPT are key indicators of liver disease in fish. Elevated plasma GOT and GPT levels suggest early hepatocyte damage [23]. Increased cell membrane permeability, which can occur with prolonged exposure to high levels of ammonia nitrogen, also leads to higher GOT and GPT levels in the serum [24,25]. Our findings showed that feeding *O. niloticus* juveniles with 5 %, 10 %, and 20 % *G. lemaneiformis* water extract had no effect on serum GOT and GPT levels. LDH plays a crucial role in vertebrate anaerobic glycolysis and is abundant in red muscle, making it important for sudden bursts of swimming activity [26]. It serves as a marker for tissue and organ damage in fish, with increased serum LDH levels observed under stress conditions, such as exposure to glyphosate [27]. CPK, present in small concentrations in plasma, including that of fish, is typically derived from normal cellular turnover. Elevated plasma CPK levels indicate changes in metabolic functions or structural damage at the tissue level [28,29]. Our study found that feeding *O. niloticus* juveniles with <20 % *G. lemaneiformis* water extract did not result in liver damage, as evidenced by normal levels of GOT, GPT, CPK, and LDH, along with histological analyses.

Immune cells produce cytokines such as IL-1β and TNF-α that trigger defense mechanisms, including the activation of immune cells

and the enhancement of phagocytosis, respiratory burst activity, and nitric oxide production against pathogens [30]. Significant upregulation of IL-1β in various fish species has been documented, indicating a systemic innate immune response to bacterial infections [31]. Algal compounds, such as polysaccharides including carrageenan, fucoidan, alginates, and β-glucan, are known to contribute to disease resistance [32]. Macroalgae such as *Ulva prolifera* and *G. lemaneiformis* have been shown to enhance the innate immune abilities of *Siganus canaliculatus* and improve resistance to *Vibrio parahaemolyticus* [33]. Quaternary alkaloids and polysaccharide fractions from *Caulerpa scalpelliformis* have been shown to immunostimulate striped murrel (*Channa striata*) and *O. niloticus*, respectively [34,35]. TNF-α is a crucial factor in stimulating the immune system. As a pleiotropic cytokine, TNF-α plays significant roles in homeostasis and disease pathogenesis and is involved in regulating adaptive immune responses [36]. Dietary supplements containing *Grateloupia acuminata* and *G. doryphore* (Halymeniaceae) nanoparticles, when administered at 24.46 ± 0.50 g to *O. niloticus* for 60 days, increased the expression of hepatic and splenic IL-8, IL-10, and TNF-α genes [37,38]. *Sarcodia suiae* water extracts elevated TNF-α expression in *O. niloticus* at 4, 8, 24, and 48 h post-injection [18]. Similarly, dietary supplementation with *Sargassum aquifolium* significantly upregulated TNF-α expression in *O. niloticus* under high stocking density conditions [37]. Consistent with these findings, our results demonstrate that feeding *O. niloticus* juveniles with 20 % *G. lemaneiformis* water extract increased the expression of IL-1β, TNF-α, and IL-10 in the liver and intestine, thereby inducing an immune response.

Diets supplemented with *Taonia atomaria* at various concentrations have been shown to induce diffuse goblet cell formation in the mucosal epithelium of the *O. niloticus* intestinal lining [39]. Histomorphometric analysis of the absorptive capacity of *O. niloticus* intestinal villi revealed improvements in villus length and goblet cell numbers following feeding with *Ulva fasciata* methanol extracts [40]. Goblet cells and mucus serve as crucial barriers, preventing pathogens from invading the mucosa and causing intestinal inflammation [41]. IL-1β stimulates the production of Tff3 and MUC2 goblet cells in response to inflammatory stress [42], whereas IL-10 promotes mucin production and corrects protein misfolding in intestinal goblet cells [43]. Consistent with these findings, a dietary supplementation of 20 % *G. lemaneiformis* water extract in *O. niloticus* juveniles enhanced intestinal goblet cell qIL-10 expression, which is involved in modulating the fish mucosal immune system.

Tryptophan metabolism encompasses several pathways, including the kynurenine and serotonin pathways. These pathways produce biologically active compounds such as serotonin, melatonin, and niacin, which are involved in various physiological functions including inflammation, metabolism, immune responses, and neurological functions [44,45]. The degradation of tryptophan into kynurenine by immune cells plays a crucial role in regulating immune responses during infections, inflammation, and pregnancy [46]. Although the importance of tryptophan metabolism in health is well-recognized, overactivation of this metabolism can also lead to disorders such as inflammatory bowel diseases [47]. In skin biopsy models, the enzyme L-kynureninase involved in tryptophan metabolism has been shown to positively correlate with novel inflammatory factors and with the presence of $CD11c^+$ dendritic cells and $CD163^+$ macrophages in lesional skin [48]. In ulcerative colitis, tryptophan metabolism through the kynurenine pathway has been found to be associated with endoscopic inflammation, as evidenced by a study of 99 patients with Mayo endoscopic subscores ranging 0–3. The kynurenic acid/tryptophan ratio and the expression of enzymes such as indoleamine 2,3-dioxygenase 1, tryptophan 2,3-dioxygenase, kynureninase, and kynurenine monooxygenase were positively correlated with endoscopic subscores [49]. Abnormal ratios of kynurenic acid/tryptophan have been linked to dysbiosis, affecting the ratios of Treg and Th17 cells [50]. Increased activation of the kynurenine pathway has also been associated with cardiovascular disease risk factors [51]. Another study reported that kynureninase-catalyzed production of kynurenine is upregulated in psoriatic skin samples from patients and animal models compared to normal skin controls; this was demonstrated through assays in the psoriatic patient samples, imiquimod-induced psoriasis-like skin inflammation in BABL/c mice, and M5-stimulated keratinocyte cell lines via immunohistochemistry [52]. Our findings indicate that dietary *G. lemaneiformis* water extract effectively downregulates kynureninase overexpression compared with the control, highlighting its role in modulating proinflammatory factors.

Proline metabolism generates electrons that produce reactive oxygen species (ROS) and initiates various downstream effects, including cell cycle blockade, autophagy, and apoptosis [53]. Proline, a nonessential amino acid, plays a crucial role in protein structure and function as well as maintaining cellular redox homeostasis. Its catabolism within cells generates ATP and ROS [54]. Proline also functions as a stress substrate, responding to stress signals and playing specialized roles in inflammation and tumorigenesis [55]. The proline metabolism pathway, including proline dehydrogenase/proline oxidase, is activated by tumor protein p53 and contributes to redox signaling, apoptosis, autophagy, and senescence [62]. In a study involving patients with hepatocellular carcinoma, patients with high levels of proline dehydrogenase or low levels of PYCR1 and ALDH18A1 have shown significantly better survival rates [61]. Metabolic pathway analyses in the liver have identified proline biosynthesis as a promoter of tumorigenesis [56]. Additionally, arginine and proline metabolism are interconnected. Arginine metabolism involves multiple enzymes that synthesize proteins, nitric oxide (NO), urea, polyamines, proline, glutamate, creatine, and agmatine. These metabolites regulate immune cell macrophages, influencing their polarization into M1 and M2 types. Activated M1 macrophages express iNOS, which converts L-arginine into NO and L-citrulline, contributing to proinflammatory responses. Conversely, anti-inflammatory M2 macrophages rely more on mitochondrial oxidative phosphorylation (OXPHOS) for energy [57]. OXPHOS machinery is involved in the efficiency and rate of ATP production, adapting to tissue-specific energy demands [58].

The Warburg effect describes a key metabolic change in innate immune cells, where glucose is predominantly converted to lactate via glycolysis even in the presence of oxygen, instead of being directed into the TCA cycle as acetyl-CoA. This metabolic shift leads to the generation of NADH, which donates electrons to the mitochondrial electron transport chain, thereby activating OXPHOS [59]. Research on glycolysis and OXPHOS has shown that although glycolysis is not essential for the differentiation of M2 macrophages, the presence of functional OXPHOS is crucial for this process [60].

PPARs are activated by fatty acids and their derivatives, many of which also signal through membrane receptors, establishing a lipid signaling network between the cell surface and the nucleus. Our proteomic analysis revealed that *G. lemaneiformis* hydrocolloids

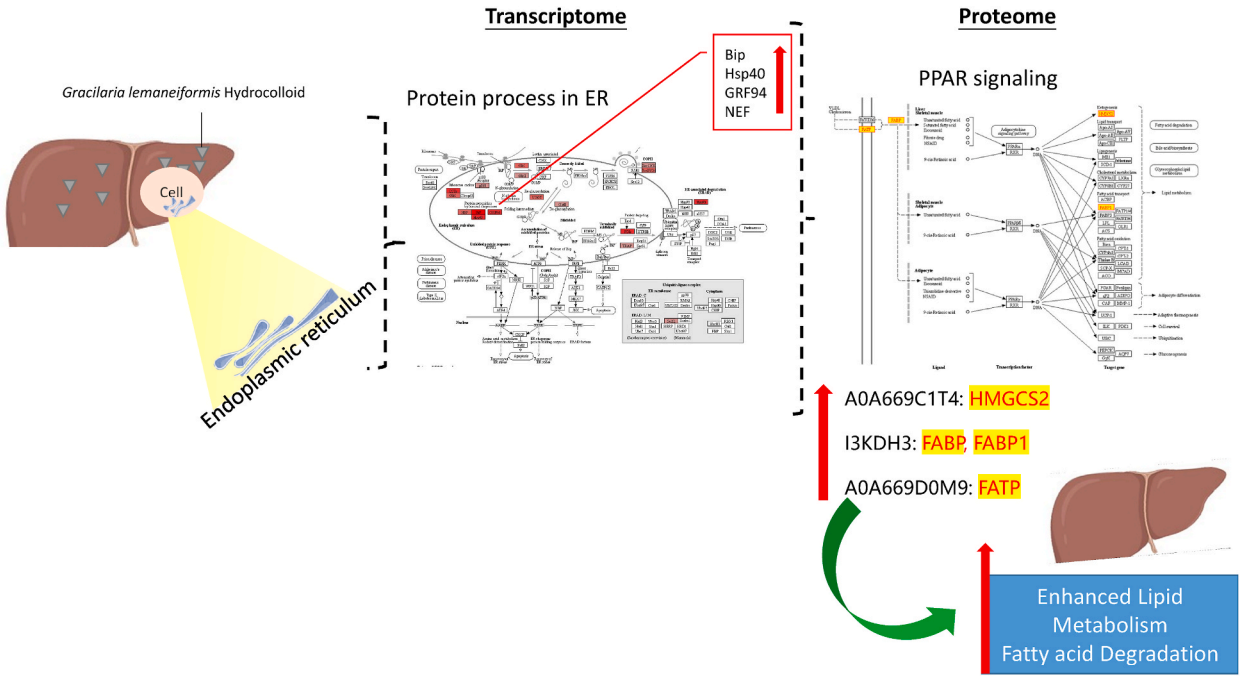

Fig. 6. Biofunctional mechanisms of *G. lemaneiformis* hydrocolloids in the intestine and liver of *O. niloticus*.

downregulated aldehyde dehydrogenase as well as the arginine and proline metabolism pathways. This finding suggests that *G. lemaneiformis* hydrocolloids play a significant role in lipid metabolism and inflammation through PPAR signaling.

8. Conclusion

G. lemaneiformis hydrocolloids did not affect the growth performance of or pose a risk to *O. niloticus*, as indicated by hematological analysis. However, the study found that a diet containing 20 % *G. lemaneiformis* hydrocolloids led to an increase in the expression of liver and intestinal cytokines, including IL-1β, TNF-α, and IL-10. Additionally, *G. lemaneiformis* hydrocolloids resulted in an increase in liver leukocyte infiltration and intestinal goblet cell counts in *O. niloticus*.

Intestine transcriptomic evidence revealed that 20 % *G. lemaneiformis* hydrocolloids upregulate the intestine PPAR signaling pathway, which plays a crucial role in linking lipid metabolism. From liver transcriptome and proteome, it also showed that 20 % *G. lemaneiformis* hydrocolloids downregulated aldehyde dehydrogenase expression and influenced arginine and proline metabolism. Conversely, levels of two key OXPHOS enzymes—mitochondrial cytochrome *c* oxidase subunit 5A and cytochrome *c* oxidase subunit 2—increased. Furthermore, KEGG pathway analysis indicated that *G. lemaneiformis* hydrocolloids upregulated HMGCS2, a mitochondrial enzyme that catalyzes the first step of ketogenesis.

Together, these findings provide evidence that 20 % *G. lemaneiformis* hydrocolloids enhanced intestine and liver lipid metabolism via PPAR signaling, as evidenced by both genomic and proteomic data illustrated in Fig. 6.

CRediT authorship contribution statement

Jia-Wei Shen: Formal analysis, Data curation. **Po-Kai Pan:** Formal analysis, Data curation. **Yin-Yu Chen:** Investigation. **Fan-Hua Nan:** Investigation. **Yu-Sheng Wu:** Writing – original draft, Investigation, Data curation.

Informed consent statement

Not applicable.

Institutional review board statement

Not applicable.

Ethical declarations

Fish care and handling procedures in the present study were approved by the Laboratory Animal Center at National Pingtung University of Science and Technology (IACUC Approval No.112-133).

Data availability

Data will be made available on request.

Funding

This study received funding from the National Pingtung University of Science and Technology and National Taiwan Ocean University.

Declaration of competing interest

The authors declare that they have no known competing financial interests or personal relationships that could have appeared to influence the work reported in this paper.

Acknowledgments

We appreciate the aquaculture practitioner Tzu-Yu Tseng (Yilan, Taiwan) for supplying *Gracilariopsis lemaneiformis*.

Appendix A. Supplementary data

Supplementary data to this article can be found online at https://doi.org/10.1016/j.heliyon.2024.e40416.

References

[1] P.S. Reel, S. Reel, E. Pearson, E. Trucco, E. Jefferson, Using machine learning approaches for multi-omics data analysis: a review, Biotechnol. Adv. 49 (2021) 107739.
[2] D.J. D'Onofrio, G. An, A, comparative approach for the investigation of biological information processing: an examination of the structure and function of computer hard drives and DNA, Theor. Biol. Med. Model. 7 (1) (2010) 3.
[3] C. Trapnell, B.A. Williams, G. Pertea, A. Mortazavi, G. Kwan, M.J. Van Baren, S.L. Salzberg, B.J. Wold, L. Pachter, Transcript assembly and quantification by RNA-Seq reveals unannotated transcripts and isoform switching during cell differentiation, Nat. Biotechnol. 28 (5) (2010) 511–515.
[4] H.C. Beck, E.C. Nielsen, R. Matthiesen, L.H. Jensen, M. Sehested, P. Finn, M. Grauslund, A.M. Hansen, O.N. Jensen, Quantitative proteomic analysis of post-translational modifications of human histones, Mol. Cell. Proteomics 5 (7) (2006) 1314–1325.
[5] S.-E. Nam, D.-Y. Bae, J.-S. Ki, C.-Y. Ahn, J.-S. Rhee, The importance of multi-omics approaches for the health assessment of freshwater ecosystems, Mol Cell Toxicol 19 (1) (2023) 3–11.
[6] Y.-J. Chen, C.-Y. Kuo, Z.-L. Kong, C.-Y. Lai, G.-W. Chen, A.-J. Yang, L.-H. Lin, M.-F. Wang, Anti-fatigue effect of a dietary supplement from the fermented by-products of Taiwan tilapia aquatic waste and monostroma nitidum oligosaccharide complex, J. Nutr. 13 (5) (2021) 1688.
[7] P.-C. Liao, Y.-L. Tsai, Y.-C. Chen, P.-C. Wang, S.-C. Liu, S.-C. Chen, Analysis of streptococcal infection and correlation with climatic factors in cultured tilapia Oreochromis spp. in Taiwan, J. Appl. Sci. 10 (11) (2020) 4018.
[8] C. Sudpraseart, P.-C. Wang, S.-C. Chen, Phenotype, genotype and pathogenicity of *Streptococcus agalactiae* isolated from cultured tilapia (Oreochromis spp.) in Taiwan, J. Fish. Dis. 44 (6) (2021) 747–756.
[9] W. Xiong, C. Guo, R.E. Gozlan, J. Liu, Tilapia introduction in China: economic boom in aquaculture versus ecological threats to ecosystems, Rev Aquac 15 (1) (2023) 179–197.
[10] G.S. Anisha, S. Padmakumari, A.K. Patel, A. Pandey, R.R. Singhania, Fucoidan from marine macroalgae: biological actions and applications in regenerative medicine, drug delivery systems and food industry, J. Bioeng. 9 (9) (2022) 472.
[11] G. Surget, V.P. Roberto, K. Le Lann, S. Mira, F. Guérard, V. Laizé, N. Poupart, M.L. Cancela, V. Stiger-Pouvreau, Marine green macroalgae: a source of natural compounds with mineralogenic and antioxidant activities, J. Appl. Phycol. 29 (1) (2017) 575–584.
[12] X. Li, Y. Gong, W. Yao, X. Chen, J. Xian, L. You, P. Fardim, Structural characterization and protective effects of polysaccharide from *Gracilaria lemaneiformis* on LPS-induced injury in IEC-6 cells, Food Chem. X 12 (2021) 100157.
[13] S. Veeraperumal, H.-M. Qiu, S.-S. Zeng, W.-Z. Yao, B.-P. Wang, Y. Liu, K.-L. Cheong, Polysaccharides from *Gracilaria lemaneiformis* promote the HaCaT keratinocytes wound healing by polarised and directional cell migration, Carbohydr. Polym. 241 (2020) 116310.
[14] E.M. Younis, A.S. Al-Quffail, N.A. Al-Asgah, A.A. Abdel-Warith, Y.S. Al-Hafedh, Effect of dietary fish meal replacement by red algae, Gracilaria arcuata, on growth performance and body composition of Nile tilapia Oreochromis niloticus, Saudi J. Biol. Sci. 25 (2) (2018) 198–203.
[15] S.V. Safavi, A.A. Kenari, M. Tabarsa, N. Esmaeili, Effect of sulfated polysaccharides extracted from marine macroalgae (*Ulva intestinalis* and *Gracilariopsis persica*) on growth performance, fatty acid profile, and immune response of rainbow trout (*Oncorhynchus mykiss*), J. Appl. Phycol. 31 (6) (2019) 4021–4035.
[16] J. Ma, T. Chen, J. Mandelin, A. Ceponis, N.E. Miller, M. Hukkanen, G.F. Ma, Y.T. Konttinen, Regulation of macrophage activation, Cell. Mol. Life Sci. 60 (11) (2003) 2334–2346.
[17] J. Zhang, Q. Wu, C. Yin, X. Jia, Z. Zhao, X. Zhang, G. Yuan, H. Hu, Q.J. Zhao, Sustained calcium ion release from bioceramics promotes CaSR-mediated M2 macrophage polarization for osteoinduction, J. Leukoc. Biol. 110 (3) (2021) 485–496.
[18] P.-T. Lee, C.-M. Wen, F.-H. Nan, H.-Y. Yeh, M.-C. Lee, Immunostimulatory effects of *Sarcodia suiae* water extracts on Nile tilapia *Oreochromis niloticus* and its resistance against *Streptococcus agalactiae*, Fish Shellfish Immunol. 103 (2020) 159–168.
[19] S. Wu, C. Duan, L. Kong, X. Tu, L. Wang, Z. Guo, J. Ye, Interleukin-10 (IL-10) participates in host defense against bacterial pathogens and promotes IgM antibody production in Nile tilapia (*Oreochromis niloticus*), Aquaculture 531 (2021) 735829.

[20] M. Stadion, C. Hackethal, K. Blume, B. Wobst, K. Abraham, C. Fechner, O. Lindtner, I. Sarvan, The first German total diet study (BfR MEAL study) confirms highest levels of dioxins and dioxin-like polychlorinated biphenyls in foods of animal origin, Food Chem. X 16 (2022) 100459.
[21] D.M. Silva, L.M.P. Valente, I. Sousa-Pinto, R. Pereira, M.A. Pires, F. Seixas, P. Rema, Evaluation of IMTA-produced seaweeds (*Gracilaria, Porphyra*, and Ulva) as dietary ingredients in Nile tilapia, *Oreochromis niloticus L.*, juveniles. Effects on growth performance and gut histology, J. Appl. Phycol. 27 (4) (2015) 1671–1680.
[22] S. Bardocz, S.W. Ewen, G. Grant, A. Pusztai, Lectins as growth factors for the small intestine and the gut, Lectins 4 (1995) 103–116.
[23] N.E. Vedel, B. Korsgaard, F.B. Jensen, Isolated and combined exposure to ammonia and nitrite in rainbow trout (*Oncorhynchus mykiss*): effects on electrolyte status, blood respiratory properties and brain glutamine/glutamate concentrations, Aquat. Toxicol. 41 (4) (1998) 325–342.
[24] Y. Xu, W. Xiao, D. Li, Z. Zou, J. Zhu, J. Han, H. Yang, Effects of chronic ammonia stress on growth and physiological function of juvenile Nile tilapia (*Oreochromis niloticus*), J S Agric 46 (2) (2015) 327–331.
[25] K. Wang, K. Li, L. Liu, C. Tanase, R. Mols, M. van der Meer, Effects of light intensity and photoperiod on the growth and stress response of juvenile Nile tilapia (*Oreochromis niloticus*) in a recirculating aquaculture system, Aquacult Fish 8 (1) (2023) 85–90.
[26] J.A. Almeida, E.L. Novelli, M.D.P. Dal Pai Silva, R.A. Júnior, Environmental cadium exposure and metabolic responses of the Nile tilapia, *Oreochromis niloticus*, Environ Pollut 114 (2) (2001) 169–175.
[27] Ü. Acar, B.E. İnanan, F.Z. Navruz, S. Yılmaz, Alterations in blood parameters, DNA damage, oxidative stress and antioxidant enzymes and immune-related genes expression in Nile tilapia (*Oreochromis niloticus*) exposed to glyphosate-based herbicide, Comp. Biochem. Physiol. C Toxicol. Pharmacol. 249 (2021) 109147.
[28] P.-K. Pan, K.-T. Wang, T.-M. Wu, Y.-Y. Chen, F.-H. Nan, Y.-S. Wu, Heat inactive *Bacillus subtilis var. natto* regulate Nile tilapia (*Oreochromis niloticus*) intestine microbiota and metabolites involved in the intestine phagosome response, Fish Shellfish Immunol. 134 (2023) 108567.
[29] S.E. Fadl, M.S. ElGohary, A.Y. Elsadany, D.M. Gad, F.F. Hanaa, N.M. El-Habashi, Contribution of microalgae-enriched fodder for the Nile tilapia to growth and resistance to infection with *Aeromonas hydrophila*, Algal Res. 27 (2017) 82–88.
[30] R.M. Reda, R. Mahmoud, K.M. Selim, I.E. El-Araby, Effects of dietary acidifiers on growth, hematology, immune response and disease resistance of Nile tilapia, *Oreochromis niloticus*, Fish Shellfish Immunol. 50 (2016) 255–262.
[31] S. Gallage, T. Katagiri, M. Endo, K. Futami, M. Endo, M. Maita, Influence of moderate hypoxia on vaccine efficacy against *Vibrio anguillarum* in *Oreochromis niloticus* (Nile tilapia), Fish Shellfish Immunol. 51 (2016) 271–281.
[32] M. Reyes-Becerril, F. Guardiola, M. Rojas, F. Ascencio-Valle, M.Á. Esteban, Dietary administration of microalgae Navicula sp. affects immune status and gene expression of gilthead seabream (*Sparus aurata*), Fish Shellfish Immunol. 35 (3) (2013) 883–889.
[33] D. Xie, X. Li, C. You, S. Wang, Y. Li, Supplementation of macroalgae together with non-starch polysaccharide-degrading enzymes in diets enhanced growth performance, innate immune indexes, and disease resistance against Vibrio parahaemolyticus in rabbitfish *Siganus canaliculatus*, J. Appl. Phycol. 31 (3) (2019) 2073–2083.
[34] R. Balasubramanian, R.D. Michael, Immunostimulatory effects of N-Oxide-Quaternary Alkaloid Fraction of a marine Chlorophycean macroalga in the striped murrel, Channa striata (Bloch), Aquac Resources 47 (2) (2016) 591–604.
[35] O. Yengkhom, K.S. Shalini, P.A. Subramani, R.D. Michael, Stimulation of non-specific immunity, gene expression, and disease resistance in Nile tilapia, *Oreochromis niloticus* (Linnaeus, 1758), by the methanolic extract of the marine macroalga, *Caulerpa scalpelliformis*, Vet. World 12 (2) (2019) 271–276.
[36] K. Li, H. Qiu, J. Yan, X. Shen, X. Wei, M. Duan, J. Yang, The involvement of TNF-α and TNF-β as proinflammatory cytokines in lymphocyte-mediated adaptive immunity of Nile tilapia by initiating apoptosis, Dev. Comp. Immunol. 115 (2021) 103884.
[37] M. Radwan, M.A. El-Sharkawy, M.A. Negm, A. Mohammadein, J.S.A. Malki, A.W. Al-Thomali, A.M. Mohamed, S. Yassir, M.A.E. Bashar, Dual effect of dietary seaweed of extract nanoparticles (GNS) with bionanocomposite cellulose acetate membranes (CA/bio-AgNps) on growth performance and health status of the Nile tilapia (*Oreochromis niloticus*): specification on feed utilization, immune system, and antiparasitic action, Front. Mar. Sci. 9 (2022) 1008397.
[38] S.S. Negm, N.E.M. Ismael, A.I. Ahmed, A.M.E. Asely, M.A.E. Naiel, The efficiency of dietary *Sargassum aquifolium* on the performance, innate immune responses, antioxidant activity, and intestinal microbiota of Nile tilapia (*Oreochromis niloticus*) raised at high stocking density, J. Appl. Phycol. 33 (6) (2021) 4067–4082.
[39] E.-S.M. Ebtehal, Effect of seaweed supplemented diets on Nile tilapia, *Oreochromis niloticus* performance, Int J Fish Aquat Sci 5 (2) (2017) 205–210.
[40] M.H. Abo-Raya, K.M. Alshehri, R.F.A. Abdelhameed, Z.I. Elbialy, S.S. Elhady, R.A. Mohamed, Assessment of growth-related parameters and immune-biochemical profile of nile tilapia (*Oreochromis niloticus*) fed dietary Ulva fasciata extract, Aquac Res 52 (7) (2021) 3233–3246.
[41] S. Yang, M. Yu, Role of goblet cells in intestinal barrier and mucosal immunity, J. Inflamm. Res. 14 (2021) 3171–3183.
[42] Y. Yu, J. Lu, K. Oliphant, N. Gupta, K. Claud, L. Lu, Maternal administration of probiotics promotes gut development in mouse offsprings, PLoS One 15 (8) (2020) e0237182.
[43] S. Cornick, M. Kumar, F. Moreau, H. Gaisano, K. Chadee, VAMP8-mediated MUC2 mucin exocytosis from colonic goblet cells maintains innate intestinal homeostasis, Nat. Commun. 10 (1) (2019) 4306.
[44] C. Xue, G. Li, Q. Zheng, X. Gu, Q. Shi, Y. Su, Q. Chu, X. Yuan, Z. Bao, J. Lu, L. Li, Tryptophan metabolism in health and disease, Cell Metab 35 (8) (2023) 1304–1326.
[45] S. Comai, A. Bertazzo, M. Brughera, S. Crotti, Tryptophan in health and disease, Adv. Clin. Chem. 95 (2020) 165–218.
[46] N. Le Floc'h, W. Otten, E. Merlot, Tryptophan metabolism, from nutrition to potential therapeutic applications, Amino Acids 41 (5) (2011) 1195–1205.
[47] S. Nikolaus, B. Schulte, N. Al-Massad, F. Thieme, D.M. Schulte, J. Bethge, A. Rehman, F. Tran, K. Aden, R. Häsler, N. Moll, G. Schütze, M.J. Schwarz, G. H. Waetzig, P. Rosenstiel, M. Krawczak, S. Szymczak, S. Schreiber, Increased tryptophan metabolism is associated with activity of inflammatory bowel diseases, Gastroenterology 153 (6) (2017) 1504–1516.
[48] J.L. Harden, S.M. Lewis, S.R. Lish, M. Suárez-Fariñas, D. Gareau, T. Lentini, L.M. Johnson-Huang, J.G. Krueger, M.A. Lowes, The tryptophan metabolism enzyme L-kynureninase is a novel inflammatory factor in psoriasis and other inflammatory diseases, J. Allergy Clin. Immunol. 137 (6) (2016) 1830–1840.
[49] M.A. Sofia, M.A. Ciorba, K. Meckel, C.K. Lim, G.J. Guillemin, C.R. Weber, M. Bissonnette, J.R. Pekow, Tryptophan metabolism through the kynurenine pathway is associated with endoscopic inflammation in ulcerative colitis, Inflamm. Bowel Dis. 24 (7) (2018) 1471–1480.
[50] X. Dagenais-Lussier, H. Loucif, C. Beji, R. Telittchenko, J.-P. Routy, J. van Grevenynghe, Latest developments in tryptophan metabolism: understanding its role in B cell immunity, Cytokine Growth Factor Rev. 59 (2021) 111–117.
[51] R. Baumgartner, M. Berg, L. Matic, K.P. Polyzos, M.J. Forteza, S.A. Hjorth, T.W. Schwartz, G. Paulsson-Berne, G.K. Hansson, U.J. Hedin, D.F.J. Ketelhuth, Evidence that a deviation in the kynurenine pathway aggravates atherosclerotic disease in humans, J. Intern. Med. 289 (1) (2021) 53–68.
[52] M. Wang, Y. Wang, M. Zhang, Q. Duan, C. Chen, Q. Sun, M. Liu, Y. Zheng, Y.J. Shao, Kynureninase contributes to the pathogenesis of psoriasis through pro-inflammatory effect, J. Cell. Physiol. 237 (1) (2022) 1044–1056.
[53] J.M. Phang, W. Liu, O. Zabirnyk, Proline metabolism and microenvironmental stress, Annu. Rev. Nutr. 30 (2010) 441–463.
[54] L.A. Vettore, R.L. Westbrook, D.A. Tennant, Proline metabolism and redox; maintaining a balance in health and disease, Amino Acids 53 (12) (2021) 1779–1788.
[55] J.M. Phang, J. Pandhare, Y. Liu, The metabolism of proline as microenvironmental stress substrate, J. Nutr. 138 (10) (2008) 2008S–2015S.
[56] Z. Ding, R.E. Ericksen, Q.Y. Lee, W. Han, Reprogramming of mitochondrial proline metabolism promotes liver tumorigenesis, Amino Acids (2021) 1–9.
[57] Y. Liu, R. Xu, H. Gu, E. Zhang, J. Qu, W. Cao, X. Huang, H. Yan, J. He, Z. Cai, Metabolic reprogramming in macrophage responses, Biomark. Res. 9 (1) (2021) 1.
[58] G. Benard, B. Faustin, E. Passerieux, A. Galinier, C. Rocher, N. Bellance, J.P. Delage, L. Casteilla, T. Letellier, R. Rossignol, Physiological diversity of mitochondrial oxidative phosphorylation, Am J Physiol Cell Physiol 291 (6) (2006) C1172–C1182.
[59] B. Kelly, L.A.J. O'Neill, Metabolic reprogramming in macrophages and dendritic cells in innate immunity, Cell Res. 25 (7) (2015) 771–784.
[60] F. Wang, S. Zhang, I. Vuckovic, R. Jeon, A. Lerman, C.D. Folmes, P.P. Dzeja, J. Herrmann, Glycolytic stimulation is not a requirement for M2 macrophage differentiation, Cell Metab 28 (3) (2018) 463–475.

[61] Z. Ding, R.E. Ericksen, N. Escande-Beillard, Q.Y. Lee, A. Loh, S. Denil, M. Steckel, A. Haegebarth, T.S.W. Wai Ho, P.J. Chow, H.C. Toh, B. Reversade, S. Gruenewald, W. Han, Metabolic pathway analyses identify proline biosynthesis pathway as a promoter of liver tumorigenesis, J. Hepatol. 72 (4) (2020) 725–735.
[62] J.M. Phang, Proline metabolism in cell regulation and cancer biology: recent advances and hypotheses, Antioxid Redox Signal 30 (4) (2019) 635–649.
[63] Rodríguez Sánchez, D.J. Canelón, V.A. Cosenza, E.N. Fissore, L.N. Gerschenson, M.C. Matulewicz, M. Ciancia, *Gracilariopsis hommersandii*, a red seaweed, source of agar and sulfated polysaccharides with unusual structures, Carbohydr. Polym. 213 (2019) 138–146.